Building Pentagons into Graphenic Structures by On-Surface Polymerization and Aromatic Cyclodehydrogenation of Phenyl-Substituted Polycyclic Aromatic Hydrocarbons

Jia Liu[1], Thomas Dienel[1], Junzhi Liu[2], Oliver Groening[1], Jinming Cai†[1], Xinliang Feng[3], Klaus Müllen[2], Pascal Ruffieux[1], and Roman Fasel[1,4]

[1] Nanotech@surfaces Laboratory, Empa - Swiss Federal Laboratories for Materials Science and Technology, 8600 Dübendorf, Switzerland

[2] Max-Planck Institut für Polymerforschung, Ackermannweg 10, 55128, Mainz, Germany

[3] Center for Advancing Electronics Dresden (cfaed) & Department of Chemistry and Food Chemistry, Technische Universität Dresden, 01062 Dresden, Germany

[4] Department of Chemistry and Biochemistry, University of Bern, Freiestrasse 3, 3012 Bern, Switzerland

ABSTRACT: 5-membered carbon rings play a crucial role in determining the geometric structure and electronic properties of carbon-based materials. Incorporating 5-membered rings into low-dimensional carbon nanomaterials with atomic precision is, however, still a challenge. Here, we report on the on-surface synthesis of a one-dimensional conjugated polymer comprising fluoranthene subunits that are obtained via surface-assisted aromatic cyclodehydrogenation of 1-phenylnaphthalene moieties within the precursor monomers. By using scanning tunneling microscopy we investigate the formation of the polymer by thermally induced dehalogenative aryl-aryl coupling and subsequent aromatic cyclodehydrogenation on a Au(111) substrate. The formed 5-membered carbon rings are directly observed with atomic resolution by non-contact atomic force microscopy. Our results show that carefully designed polyphenylene precursors can be used for the rational fabrication of 5-membered rings in the bottom-up synthesis of carbon-based nanomaterials, and thus add a further tool to the emerging field of on-surface synthesis.

INTRODUCTION

On-surface synthesis has proven to be a promising method for the bottom-up fabrication of novel low dimensional nanomaterials with atomic precision.[1, 2] It makes use of precursor molecules as building blocks that can be thermally activated after vacuum deposition onto a metallic substrate to form extended, covalently bonded one- and two-dimensional nanostructures. Varying the chemical structure of the molecular precursors, a large range of nanomaterials have been fabricated.[3-10] Among these, owing to the soaring interest in graphene related carbon nanomaterials, various sp^2 carbon nanostructures such as graphene nanoribbons,[11, 12] graphene quantum dots,[13] or porous graphene[14] have been fabricated by using rationally designed molecular building blocks.

Pentagonal rings introduced into hexagonal sp^2 carbon networks play a crucial role in determining the geometric structure as well as the electronic properties of the corresponding nanomaterial. It is well known that the curvature of some carbon allotropes such as fullerenes and nanocones is induced by pentagons[15]. More generally, pentagons together with other polygonal structures in graphene are classified as topological defects, such as Stone–Wales defect, 5-7 defect, 5-8-5 defect and so on.[16-18] In addition to their geometrical properties, topologic defects and pentagons in particular are predicted to be highly interesting for the band structure engineering of sp^2 bonded carbon materials.[19] Since pentagons and other odd-numbered non-hexagonal polygons disrupt the A-B bonding topology of the bipartite hexagonal graphene network, such topological defects induce novel electronic features. For example, by introducing pentagon and heptagon defects, carbon nanotube intramolecular junctions were fabricated with rectifying properties,[20] and pentagonal topological defects were reported to exhibit magnetic properties.[21] Furthermore, pentagraphene, a 2D carbon network composed of pentagons only, was predicted to be stable with unusual mechanical and electronic properties,[22] and carbon networks made of fused pentagons with large dodecagonal pores were found to exhibit ferromagnetic properties.[23] Although pentagon incorporation may impart the resulting carbon-based nanostructures with unique electronic features, little attention has been paid hitherto to the creation of pentagonal bond configurations by on-surface synthesis.

Here we present an on-surface synthesis of the aromatic cyclodehydrogenation of 1-phenylnaphthalene **1** into fluoranthene **2** that was originally reported by Orchin et al. in 1947 (Scheme 1) as a versatile strategy to introduce pentagonal bond configurations.[24] We designed the dibromo-terminated molecular building block, 5,12-bis(4-bromophenyl)benzo[*k*]tetraphene **3**, incorporating two - 1-phenylnaphthalene subunits. Upon thermal activation on Au(111) and under ultrahigh vacuum conditions, **3** undergoes dehalogenation and polymerization into a linear poly(5,12-diphenylbenzo[*k*]tetraphene) (**4)** (Scheme 1). Subsequent annealing at higher temperatures leads to cyclodehydrogenation within the 1-phenylnaphthalene subunit transforming it to

fluoranthene type subunit **2** under formation of a pentagonal carbon ring. Altogether, the resulting polymer poly(fluoreno[1,9-*kl*]indeno[1,2,3-*de*]tetraphene) (**5**) is the product of a thermally induced surface-assisted two-step reactions. We employ scanning tunneling microscopy (STM) and non-contact atomic force microscopy (nc-AFM) to investigate the adsorption and self-assembly of the molecular precursor **3** on Au(111), the intermediate steps of the polymer formation, and to confirm the pentagonal ring closure for polymer **5**.

Scheme 1. Formation of five-membered carbon rings by aromatic cyclodehydrogenation: The 'classical' example of fluoranthene (1→2), and the on-surface synthesis of polymer 5 in a thermally induced two-step reaction from precursor 3.

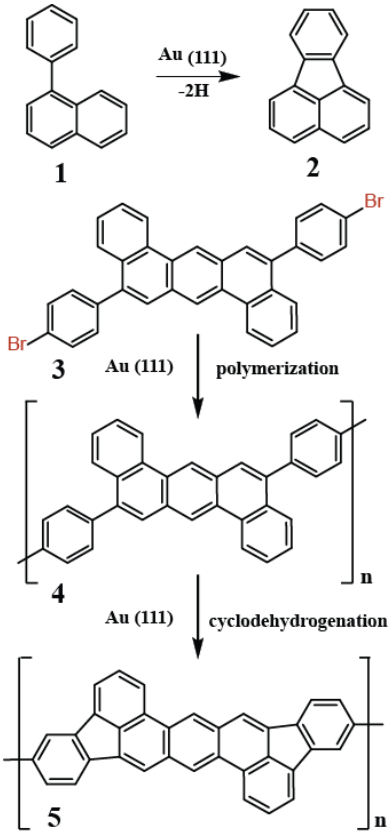

RESULTS and DISCUSSION

Figure 1a shows an overview STM image after deposition of molecule **3** on a Au(111) surface held at room temperature (RT). One can readily distinguish the usual $22 \times \sqrt{3}$ herringbone reconstruction of the gold substrate and three types of equally high islands. The monomers within the islands can be identified by the z-shape of their benzo[*k*]tetraphene core structure and the bright protrusions of the terminal bromophenyl units. Because molecule **3** is prochiral,[25, 26] two enantiomers labeled here as R and S are obtained upon adsorption on the surface, as shown in Figure 1b. The three different types of domains seen in Fig. 1a can be identified as enantiopure R and enantiopure S domains, as well as a racemic R&S domain consisting of alternating rows of R and S enantiomers (see Fig. 1c, with structural models superposed). The unit cell parameters of the R&S domain are: a = 1.5 nm, b = 2.7 nm, α = 58°, as outlined in Figure 1c. In contrast, Figure 1d highlights the enantiopure domains solely containing R or S monomers, respectively. The unit cell parameters of the domains R and S are analogous, as to be expected for mirror domains, and indicated in Figure 1d, with a = 1.3 nm, b = 1.8 nm, α = 87°.

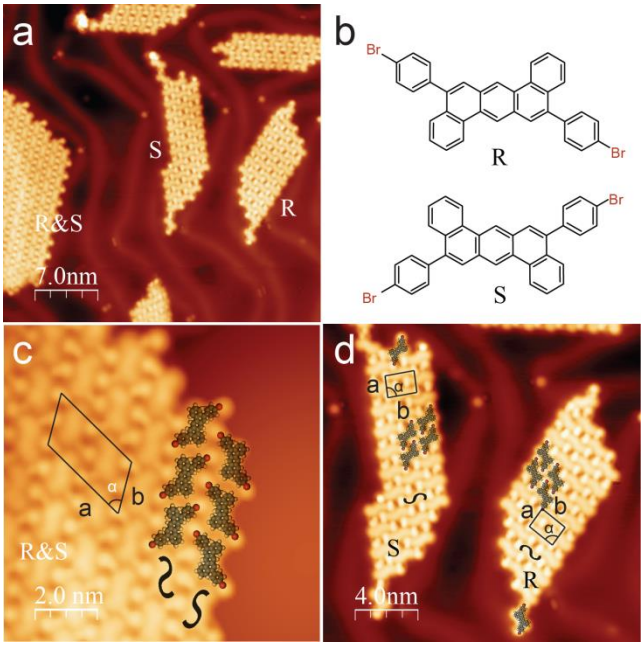

Figure 1. Room-temperature self-assembly of monomer **3** on Au(111). a) Large scale STM image of molecule **3** deposited at room temperature on Au(111). b) Illustration of the adsorption induced mirror symmetry breaking of 5,12-bis(4-bromophenyl)benzo[*k*]tetraphene. c) Zoom-in STM image of the racemic R&S domain. d) Zoom-in STM image of enantiopure R and S domains. Tunneling conditions (current setpoint/bias voltage): 60 pA/-0.8 V (a, c, d).

Neither of the self-assembled structures exhibits intermolecular arrangements for straight-forward (topochemical) dehalogenation-based coupling reactions, and an increase of mobility of the monomers upon dehalogenation is thus required. Figure 2a displays a large scale STM image of **3** deposited on Au(111) and subsequent annealing for 15 min at 200°C. Between RT and 200°C, monomers undergo dehalogenation and form linear, short oligomers of structure **4** with an average length of about 5 nm (Figures 2a and b). Figure 2b also reveals that the oligomers are closely packed, with semi-bright protrusions between them that we attribute to bromines that remain on the Au(111) substrate after dehalogenation.

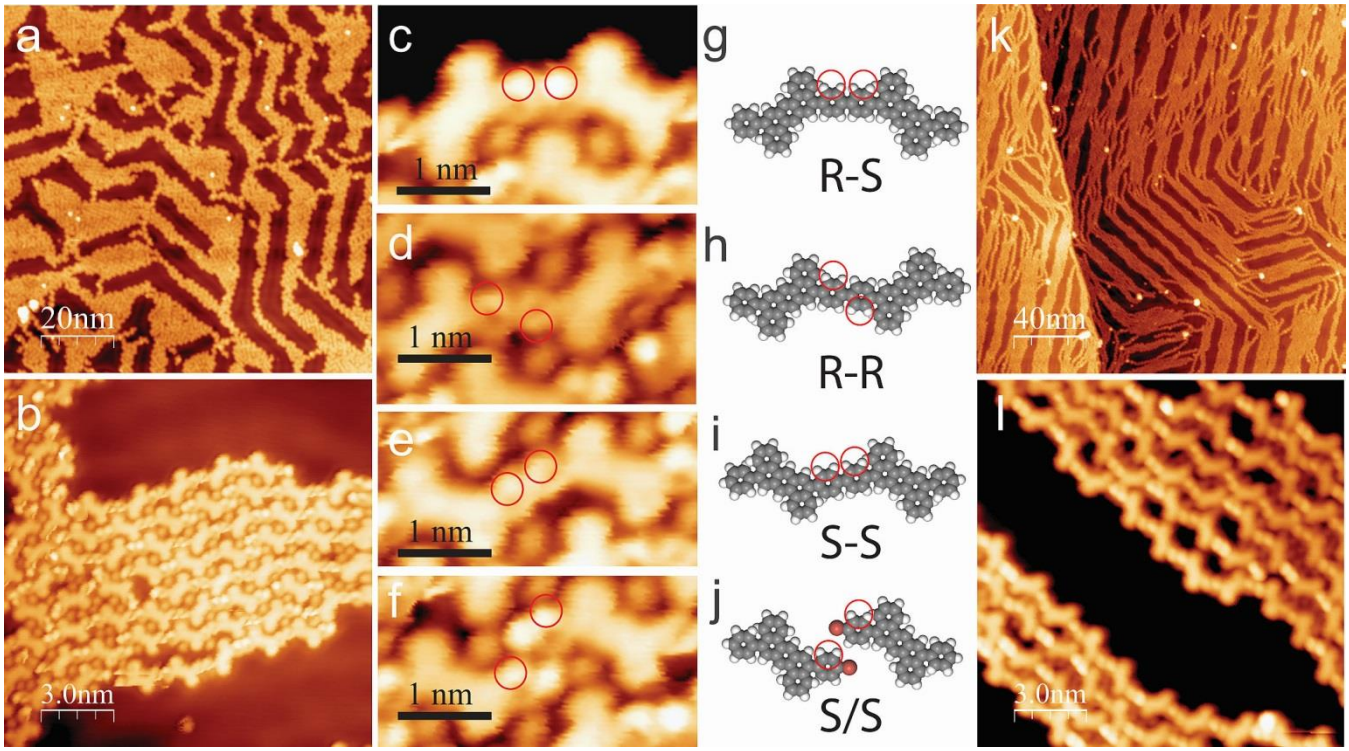

Figure 2. a) Large scale STM image of oligomers of **4** after annealing **3** for 15 min at 200℃ on Au(111). b) Zoom-in STM image of oligomers of **4**. c) - f) Zoom-in STM images of the four typical dimer motifs that are observed. g) - j) Molecular models of the four dimer motifs. The rotated parts caused by steric hindrance of hydrogen atoms are indicated with red circles, corresponding to the ones in c) - j). k) Large scale STM image of polymer **4** after annealing at 300℃ on Au(111). l) Zoom-in STM image of polymer **4**. Tunneling conditions (current setpoint/bias voltage): (a) 100 pA/0.7 V; (b) 60 pA/0.1 V; (c) 60 pA/0.1 V; (d) 60 pA/0.1 V; (e) 60 pA/0.1 V; (f) 60 pA/0.1 V; k) 60 pA/-1.2 V; (l) 60 pA/-1.0 V.

Since **3** is present on the surface as a racemic mixture of the R and S enantiomers, three different diastereoisomers can be formed upon aryl-aryl coupling of two monomers. Figures 2c-2e are high resolution STM images of the three typical dimer structures that can be attributed to R-S, R-R and S-S diastereoisomers (molecular models in Figure 2g-i). The distance of the two connected central phenyls is about 4 Å in all three cases, indicating covalent bonding. A few remaining unreacted monomers with bromine atoms still attached are also resolvable as shown in Figure 2f (molecular model in Figure 2j). Adjacent phenyl groups (indicated by red circles) are twisted, *i.e.*, rotated out of the (surface) plane of the z-shaped aromatic core of **3**. The apparent height difference within the phenyl rings of about 0.4 Å (reflecting the out-of-plane rotation) is caused by steric hindrance of nearby hydrogen atoms.[11, 13] It should be noted that this kind of steric hindrance weakens the corresponding C-H bonds and thus lowers the barrier to thermally induced on-surface cyclodehydrogenation.[13, 27, 28]

Given that samples annealed to 200°C are not fully polymerized, we further annealed to 300°C. Indeed, significantly longer polymer strands were obtained, as shown in Figure 2k. Notably, most of the polymer strands are longer than 200 nm, which is significantly longer than what has been reported for 1D polymers fabricated via on-surface synthesis so far (on the order of 100 nm).[29-31] The surprisingly long polymers obtained here may be attributed to several factors. Firstly, after dehalogenation of **3** the radical position is maximally exposed, *i.e.* there is no steric hindrance to aryl coupling. Secondly, the temperature difference between dehalogenation (<200°C) and cyclodehydrogenation (which requires temperatures even higher than the 300°C for the formation of the long polymer) is large, and the two reaction steps are thus well separated. This minimizes the release of hydrogen via premature cyclodehydrogenation during the polymerization step, and thus minimizes radical passivation by the released hydrogen, which would stop further polymerization.[32] Thirdly, the polymer **4**, with its twisted biphenyl-bridged benzo[*k*]tetraphene structure (see Figure 2k,l) is expected to be structurally flexible (as is reflected in Fig. 2k where polymer strands are seen to closely follow the herringbone reconstruction of the Au(111) substrate surface), which increases the probability of two oligomer ends to meet and bind to each other in the polymerization step.

STM images such as the one shown in Fig. 2l allow identifying the constituting enantiomeric units along the backbone of polymer **4**. In order to understand whether there is a correlation in the sequence of enantiomeric units (which would reflect unequal probabilities for homo- *vs.* heterochiral coupling), we analyzed several polymer strands containing a total of more than 600 units (Supporting Figure S1). Comparison with statistical simulations reveals an entirely random distribution of enantiomers along the polymer (for calculation details see Supporting Information), and thus no enantiomeric coupling selectivity.

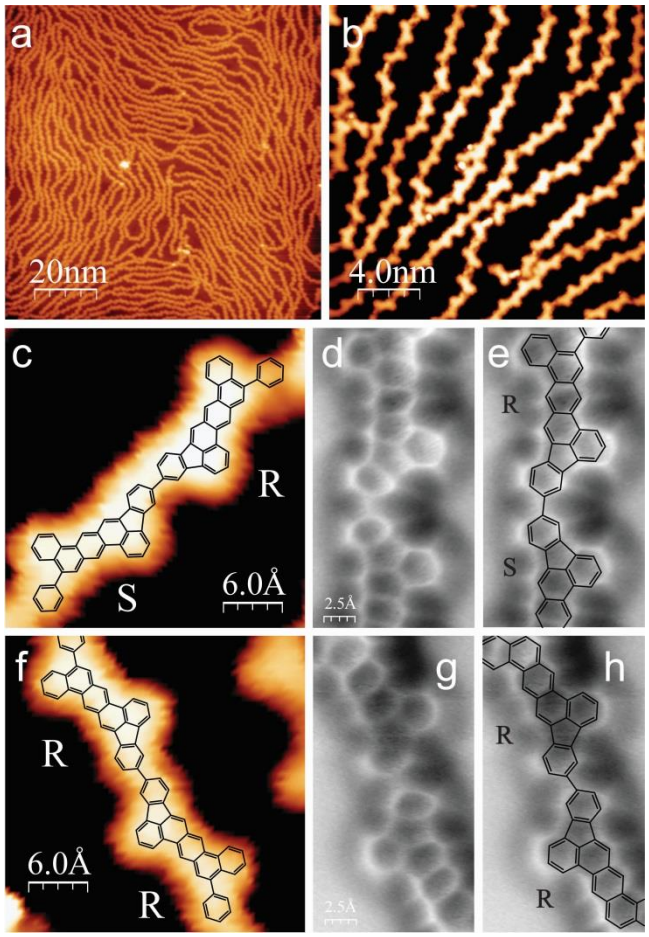

Figure 3. a) Large scale STM image of polymer **5** after annealing polymer **4** at 400℃ on Au(111). b) Zoom-in STM image of polymer **5**. c) and f) Zoom-in STM images of two typical isomeric dimer segments after aromatic cyclodehydrogenation, with the corresponding molecular models overlaid as a guide to the eye. d) and g) Constant-height frequency shift nc-AFM images of polymer **5** acquired with a CO-functionalized tip. e) and h) The same images as d) and g) with the molecular models overlaid as a guide to the eye. Tunneling conditions (current setpoint/bias voltage): (a) 100 pA/1.0 V; (b) 60 pA/-0.5 V; (c) 60 pA/-0.5 V; (f) 60 pA/-0.5 V.

In order to induce cyclodehydrogenation we further annealed the sample to 400°C. Figure 3a shows a large scale STM image of the resulting polymer **5** on Au(111). In contrast to the situation at 200°C and 300°C (Figure 2) where the polymer strands appeared in bundles with interstitial bromine atoms, the polymer strands are now well separated from each other and bromine atoms have desorbed from the surface.[33] The close-up STM image in Figure 3b also reveals that most of the twisted (rotated out-of-plane) phenyl rings are no longer observed. Focusing on typical segments formed during dehalogenation (cf. Figure 2h-i), one can see that they now appear entirely planar (Figure 3c and 3f), which is a first indication that pentagonal sp2-carbon rings were formed, removing the steric hindrance of the hydrogen atoms discussed above. To unambiguously determine the structure of the created polymers we employ nc-AFM with CO-functionalized tips.[34-39] From Figure 3d and 3g it can be clearly seen that the phenyl groups are fused to the benzo[*k*]tetraphene core by incorporating pentagonal, forming fluoreno[1,9-*kl*]indeno[1,2,3-*de*]tetraphene subunits (see overlaid structural models in Figure 3e and 3h). Notably, the entire ring system of the polymer shows uniform frequency shifts in constant height nc-AFM images, confirming that polymer **5** indeed consists of planar fluoranthene units.

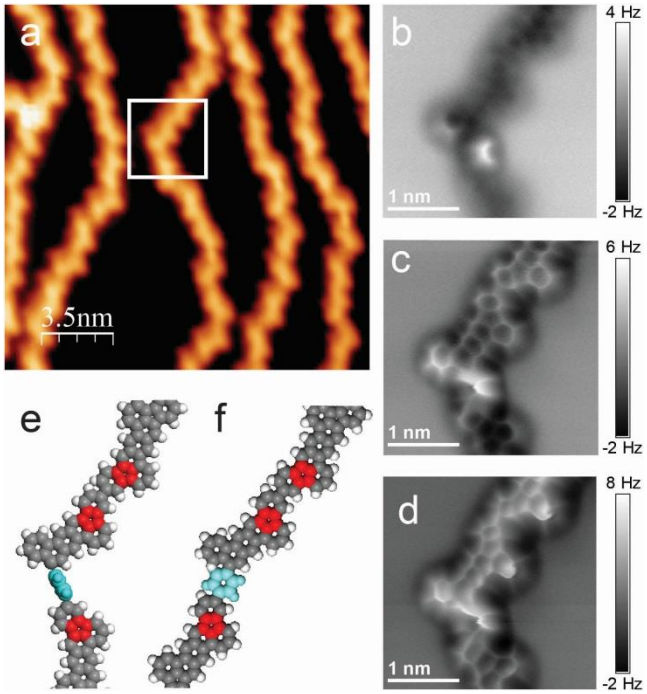

Figure 4. Cyclodehydrogenation induced strain. a) Overview STM image of (partially) cyclodehydrogenated polymer **5** (100 pA/0.2 V). b) to d) Frequency shift nc-AFM images of segment highlighted in (a) acquired in constant-height mode with a CO-functionalized tip at different relative setpoints *z* (0 pm (b), -80 pm (c) and -100 pm (d)). e) Molecular model of the segment under investigation in (b,c,d). d) Fully relaxed structure of the same segment.

Careful analysis of the STM images reveals that not all of the phenyl rings in the long polymer strands have undergone cyclodehydrogenation – around ⅓ of them have not reacted and remain twisted out-of-plane (Figure 3b). We attribute this incomplete transformation to the fact that the cyclodehydrogenation requires a significant structural relaxation of the molecular units, and consequently a relaxation of the entire polymer chain, as illustrated in Supplementary Figure S4. While such structural relaxation is not significant obstacle in a (three-dimensional) solution environment, on a (two-dimensional) solid substrate surface the confined space and the occasional interconnections between polymer strands impose constraints that may prevent sufficient relaxation and lead to the build-up of significant strain. Figure 4 shows an overview STM image and corresponding constant-height nc-AFM images of a strongly bent polymer segment (white box in Figure 4a). The sequence of frequency shift images acquired at decreasing tip-sample distance (Figure 4b to 4d) first allows the identification of an upright oriented phenyl ring (bright feature in Figure 4b, marked in blue in Figure 4e), and for smaller tip-sample distances then reveals the entire backbone of the polymer (Figure 4c,d). Once the CO-functionalized tip is too close to the surface (Figure 4d) the rings of the planar backbone undergo a contrast inversion and their centers tend to appear bright.[40] Additionally, the CO molecule at the tip

shows a strong interaction with the upright oriented phenyl ring, which leads to a distorted imaging of this part of the polymer (see also the case of two consecutive upright oriented phenyl rings in Supporting Figure S5).[35, 41] From the three nc-AFM images we thus learn that the selected polymer segment comprises three pentagonal rings (marked in red in Figure 4e) and one unreacted phenyl ring that is rotated out-of-plane (marked in blue in Figure 4e). The orientation of the distorted phenyl ring and its binding configuration to the neighboring planar parts of the polymer are clearly far from what is required for successful cyclodehydrogenation (compare relaxed model in Figure 4f).

CONCLUSION

In summary, we have shown by STM and nc-AFM that thermally induced aromatic cyclodehydrogenation on a solid substrate was successfully used to incorporate pentagonal carbon rings into a linear polymer by introducing 1-phenylnaphthalene subunits into the molecular building blocks. The fact that the thus formed pentagons are not fully coordinated by hexagons (e.g. as in a fullerene) preserves the planarity of the whole structure. This is an important feature in view of possible subsequent on-surface chemical additions or modification, where planarity might be required to maintain regularity of the ribbon structure. We consider that further modifications of the molecular precursors encompassing 1-phenylnaphthalene subunits will allow the on-surface synthesis of widely diverse products. Future investigations will focus on integrating pentagons into atomically precise graphene nanoribbons.[11]

Experimental Methods

Synthesis of 5,12-bis(4-bromophenyl)benzo[*k*]tetraphene (3).

A solution of 2',5'-Bis((Z)-4-bromostyryl)-1,1':4',1''-terphenyl (500 mg, 0.87 mmol) and iodine (500 mg, 2 mmol) in toluene (400 mL) and propylene oxide (100 mL) was irradiated in a standard immersion well photoreactor with 360nm high pressure mercury vapor lamps (8x360nm) for 8 h. The reaction mixture was then washed with aqueous sodium thiosulfate, water, brine and dried over anhydrous $MgSO_4$. The solvent was removed under vacuum and the residue was purified by silica gel column chromatography using dichloromethane (DCM) /hexane (1/5, v/v) as eluent to give the title compound (300 mg) as a white solid in 60.5% yield. ^{1}H-NMR (THF-d, 500 MHz): δ 9.27 (s, 1H), 8.97 (d, 1H), 7.88 (s, 1H), 7.76 (d, 1H), 7.64-7.62 (m, 3H), 7.52-7.43 (m, 3H); ^{13}C-NMR (THF-d, 125 MHz): 140.95, 138.77, 132.70, 132.46, 131.95, 131.72, 131.56, 130.24, 129.00, 127.90, 127.79, 127.46, 124.32, 123.31, 122.39. FD-MS (8 KV): *m/z*=588.9. HR-MS (MALDI): *m/z* = 587.9890, calcd. for $C_{34}H_{20}Br_2$: *m/z* = 587.9911.

STM and nc-AFM measurements.

Sample preparation, STM and nc-AFM measurements were performed in an ultrahigh vacuum system using an Omicron LT-STM. The Au(111) substrate was cleaned by standard argon sputtering/annealing cycles before deposition of the monomers. 5,12-bis(4-bromophenyl)-benzo[*k*]tetraphene was deposited from a homemade evaporator at 320°C at a rate of about 0.1 ML min^{-1} onto the sample, which was held at room temperature. STM and nc-AFM analysis were performed at 5 K. nc-AFM measurements were performed with a tungsten tip attached to a tuning fork sensor (ScientaOmicron). The tip was functionalized with a single CO molecule, picked up from the previously dosed surface.[42] The sensor was driven close to its resonance frequency (~ 23570 Hz) with a constant amplitude of approximately 70 pm. The shift in the resonance frequency of the tuning fork (with the attached CO-functionalized tip) was recorded in constant height mode (Omicron Matrix electronics and HF2Li PLL by Zürich Instruments). The STM and nc-AFM images were analyzed using WSxM.[43]

ASSOCIATED CONTENT

Supporting Information. Statistical analysis of polymer chains, additional nc-AFM images, synthesis details, crystallographic data, NMR, and MS. This material is available free of charge via the Internet at http://pubs.acs.org.

AUTHOR INFORMATION

Corresponding Author

* roman.fasel@empa.ch

Present Addresses

† Faculty of Materials Science and Engineering, Kunming University of Science and Technology, 650000, Kunming, China.

ACKNOWLEDGMENT

This work was supported by the Swiss National Science Foundation, the Office of Naval Research BRC Program, the European Research Council (grant NANOGRAPH), the DFG Priority Program SPP 1459, the Graphene Flagship (No. CNECT-ICT-604391), and the European Union Projects UPGRADE, GENIUS, and MoQuaS.

REFERENCES

(1) Lindner, R.; Kühnle, A. *ChemPhysChem* **2015**, *16*, 1582.

(2) Mendez, J.; Lopez, M. F.; Martin-Gago, J. A. *Chem. Soc. Rev.* **2011**, *40*, 4578.

(3) Yang, B.; Björk, J.; Lin, H.; Zhang, X.; Zhang, H.; Li, Y.; Fan, J.; Li, Q.; Chi, L. *J. Am. Chem. Soc.* **2015**, *137*, 4904.

(4) Riss, A.; Wickenburg, S.; Gorman, P.; Tan, L. Z.; Tsai, H.-Z.; de Oteyza, D. G.; Chen, Y.-C.; Bradley, A. J.; Ugeda, M. M.; Etkin, G.; Louie, S. G.; Fischer, F. R.; Crommie, M. F. *Nano Lett.* **2014**.

(5) Lindner, R.; Rahe, P.; Kittelmann, M.; Gourdon, A.; Bechstein, R.; Kühnle, A. *Angew. Chem., Int. Ed.* **2014**, *53*, 7952.

(6) Eichhorn, J.; Strunskus, T.; Rastgoo-Lahrood, A.; Samanta, D.; Schmittel, M.; Lackinger, M. *Chem. Commun.* **2014**.

(7) Sun, Q.; Zhang, C.; Li, Z.; Kong, H.; Tan, Q.; Hu, A.; Xu, W. *J. Am. Chem. Soc.* **2013**, *135*, 8448.

(8) Gao, H.-Y.; Wagner, H.; Zhong, D.; Franke, J.-H.; Studer, A.; Fuchs, H. *Angew. Chem., Int. Ed.* **2013**, *52*, 4024.

(9) Abel, M.; Clair, S.; Ourdjini, O.; Mossoyan, M.; Porte, L. *J. Am. Chem. Soc.* **2011**, *133*, 1203.

(10) Liu, J.; Ruffieux, P.; Feng, X.; Müllen, K.; Fasel, R. *Chem. Commun.* **2014**, *50*, 11200.

(11) Cai, J.; Ruffieux, P.; Jaafar, R.; Bieri, M.; Braun, T.; Blankenburg, S.; Muoth, M.; Seitsonen, A. P.; Saleh, M.; Feng, X.; Müllen, K.; Fasel, R. *Nature* **2010**, *466*, 470.

(12) Chen, Y.-C.; de Oteyza, D. G.; Pedramrazi, Z.; Chen, C.; Fischer, F. R.; Crommie, M. F. *ACS Nano* **2013**, *7*, 6123.

(13) Treier, M.; Pignedoli, C. A.; Laino, T.; Rieger, R.; Muellen, K.; Passerone, D.; Fasel, R. *Nat. Chem.* **2011**, *3*, 61.

(14) Bieri, M.; Treier, M.; Cai, J.; Ait-Mansour, K.; Ruffieux, P.; Groning, O.; Groning, P.; Kastler, M.; Rieger, R.; Feng, X.; Mullen, K.; Fasel, R. *Chem. Commun.* **2009**, 6919.

(15) Evstafyev, V. K. *Fullerenes, Nanotubes and Carbon Nanostructures* **2012**, *21*, 125.

(16) Rasool, H. I.; Ophus, C.; Zettl, A. *Adv. Mater.* **2015**, *27*, 5771.

(17) Meyer, J. C.; Kisielowski, C.; Erni, R.; Rossell, M. D.; Crommie, M. F.; Zettl, A. *Nano Lett.* **2008**, *8*, 3582.

(18) Wang, Z.; Zhou, X.-F.; Zhang, X.; Zhu, Q.; Dong, H.; Zhao, M.; Oganov, A. R. *Nano Lett.* **2015**, *15*, 6182.

(19) Charlier, J. C. *Acc. Chem. Res.* **2002**, *35*, 1063.

(20) Yao, Z.; Postma, H. W. C.; Balents, L.; Dekker, C. *Nature* **1999**, *402*, 273.

(21) Kusakabe, K.; Wakabayashi, K.; Igami, M.; Nakada, K.; Fujita, M. *Mol. Cryst. Liq. Cryst. Sci. Technol., Sect. A* **1997**, *305*, 445.

(22) Zhang, S.; Zhou, J.; Wang, Q.; Chen, X.; Kawazoe, Y.; Jena, P. *Proc. Natl. Acad. Sci. U.S.A.* **2015**, *112*, 2372.

(23) Mina, M.; Susumu, O. *Appl. Phys. Express* **2013**, *6*, 095101.

(24) Orchin, M.; Reggel, L. *J. Am. Chem. Soc.* **1947**, *69*, 505.

(25) Ernst, K. H. *Surf. Sci.* **2013**, *613*, 1.

(26) Chen, T.; Wang, D.; Wan, L.-J. *Natl. Sci. Rev.* **2015**, 2, 205.

(27) Björk, J.; Hanke, F. *Chem.-Eur. J.* **2014**, *20*, 928.

(28) Wiengarten, A.; Lloyd, J. A.; Seufert, K.; Reichert, J.; Auwarter, W.; Han, R. Y.; Duncan, D. A.; Allegretti, F.; Fischer, S.; Oh, S. C.; Saglam, O.; Jiang, L.; Vijayaraghavan, S.; Ecija, D.; Papageorgiou, A. C.; Barth, J. V. *Chem.-Eur. J.* **2015**, *21*, 12285.

(29) Lafferentz, L.; Ample, F.; Yu, H.; Hecht, S.; Joachim, C.; Grill, L. *Science* **2009**, *323*, 1193.

(30) Gahl, C.; Brete, D.; Leyssner, F.; Koch, M.; McNellis, E. R.; Mielke, J.; Carley, R.; Grill, L.; Reuter, K.; Tegeder, P.; Weinelt, M. *J. Am. Chem. Soc.* **2013**, *135*, 4273.

(31) Adisoejoso, J.; Lin, T.; Shang, X. S.; Shi, K. J.; Gupta, A.; Liu, P. N.; Lin, N. *Chem.-Eur. J.* **2014**, *20*, 4111.

(32) Talirz, L.; Söde, H.; Cai, J.; Ruffieux, P.; Blankenburg, S.; Jafaar, R.; Berger, R.; Feng, X.; Müllen, K.; Passerone, D.; Fasel, R.; Pignedoli, C. A. *J. Am. Chem. Soc.* **2013**, *135*, 2060.

(33) Bronner, C.; Björk, J.; Tegeder, P. *J. Phys. Chem. C* **2015**, *119*, 486.

(34) Gross, L.; Mohn, F.; Moll, N.; Liljeroth, P.; Meyer, G. *Science* **2009**, *325*, 1110.

(35) Gross, L.; Mohn, F.; Moll, N.; Meyer, G.; Ebel, R.; Abdel-Mageed, W. M.; Jaspars, M. *Nat. Chem.* **2010**, *2*, 821.

(36) Albrecht, F.; Neu, M.; Quest, C.; Swart, I.; Repp, J. *J. Am. Chem. Soc.* **2013**, *135*, 9200.

(37) de Oteyza, D. G.; Gorman, P.; Chen, Y. C.; Wickenburg, S.; Riss, A.; Mowbray, D. J.; Etkin, G.; Pedramrazi, Z.; Tsai, H. Z.; Rubio, A.; Crommie, M. F.; Fischer, F. R. *Science* **2013**, *340*, 1434.

(38) Moreno, C.; Stetsovych, O.; Shimizu, T. K.; Custance, O. *Nano Lett.* **2015**, *15*, 2257.

(39) Zhang, J.; Chen, P.; Yuan, B.; Ji, W.; Cheng, Z.; Qiu, X. *Science* **2013**, *342*, 611.

(40) Hapala, P.; Kichin, G.; Wagner, C.; Tautz, F. S.; Temirov, R.; Jelínek, P. *Phys. Rev. B* **2014**, *90*, 085421.

(41) Albrecht, F.; Pavliček, N.; Herranz-Lancho, C.; Ruben, M.; Repp, J. *J. Am. Chem. Soc.* **2015**, *137*, 7424.

(42) Bartels, L.; Meyer, G.; Rieder, K. H.; Velic, D.; Knoesel, E.; Hotzel, A.; Wolf, M.; Ertl, G. *Phys. Rev. Lett.* **1998**, *80*, 2004.

(43) Horcas, I.; Fernández, R.; Gómez-Rodríguez, J. M.; Colchero, J.; Gómez-Herrero, J.; Baro, A. M. *Rev Sci Instrum* **2007**, *78*, 013705.

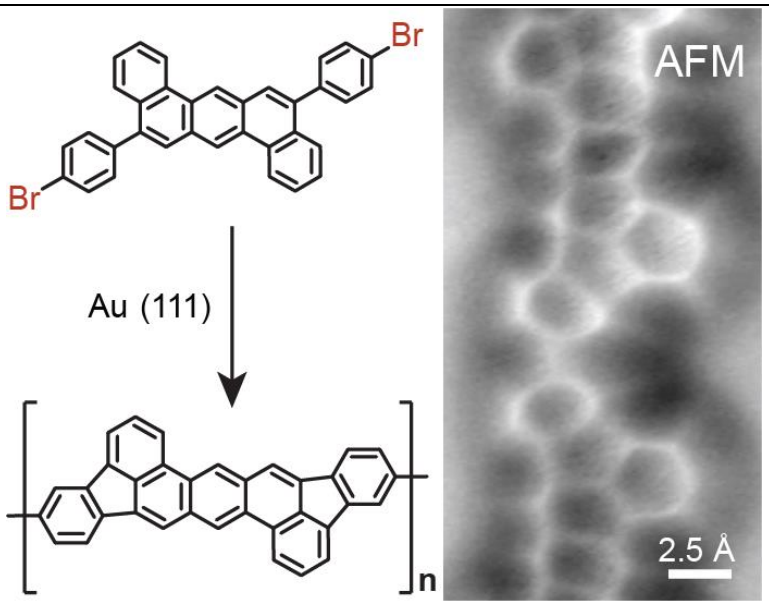
Br
Br
Au (111)
n
AFM
2.5 Å